OFFICE OF SCIENTIFIC RESEARCH & DEVELOPMENT
NATIONAL DEFENSE RESEARCH COMMITTEE.
DIVISION SIX-SECTION 6.1

WATER TUNNEL TESTS
OF THE
M7, 2.36" A.T. ROCKET

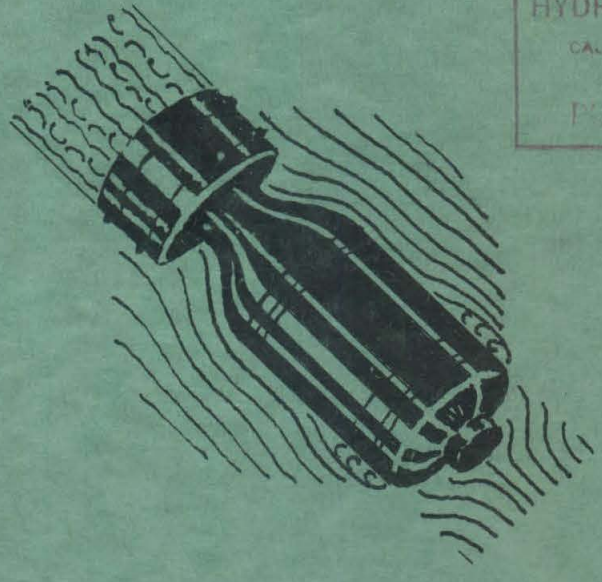

THE HIGH SPEED WATER TUNNEL
CALIFORNIA INSTITUTE OF TECHNOLOGY
PASADENA, CALIFORNIA.

SECTION № 6.1-Sr-207-276

COPY № 50

~~(CONFIDENTIAL)~~

OFFICE OF SCIENTIFIC RESEARCH AND DEVELOPMENT
NATIONAL DEFENSE RESEARCH COMMITTEE
DIVISION SIX — SECTION 6.1

MEMORANDUM ON WATER TUNNEL TESTS OF THE M-7, 2.36" A. T. ROCKET SHOWING COMPARISON OF PERFORMANCE WITH A FOLDING FIN TAIL A SHROUD RING TAIL TWO HEMISPHERICAL OGIVE NOSES OF DIFFERENT PROFILE AND A CONICAL POINTED NOSE

BY

ROBERT T. KNAPP
OFFICIAL INVESTIGATOR

THE HIGH SPEED WATER TUNNEL
AT THE
CALIFORNIA INSTITUTE OF TECHNOLOGY
HYDRAULIC MACHINERY LABORATORY
PASADENA, CALIFORNIA

Section No. 6.1-sr-207-276
HML Rep. No. ND-11.3
Copy No.

June 26, 1943

ABSTRACT

This report covers water tunnel tests of a 2.36" rocket projectile with several variations in profile of nose and with two types of tail; a folding fin tail and a fixed shroud ring tail. The hydrodynamic forces, drag, cross wind force, and moment, acting on the projectile, were measured and the locations of the center-of-pressure were calculated for the various combinations of noses and tails and at various velocities and yaw angles.

CONCLUSIONS

Figures 1, 2, and 3 show the two hemispherical noses in combination with the folding fin tail and the shroud ring tail.

Of the two hemispherical ogive noses, the larger diameter nose has a lower drag, regardless of the type of tail. The conical pointed nose, with either tail, has less drag than either of the ogive noses.

Stability, with either nose, is better with the folding fin tail than with the shroud ring tail. With the folding fin tail the two hemispherical noses have equal stability and the conical pointed nose somewhat better stability. With the shroud ring tail, the stability is less than with the fin tail and is practically the same with any one of the noses.

The shroud ring tail appears to offer advantages over the folding fin tail in simplicity, uniformity of manufacture, less possibility of damage in handling, and freedom from possible damage due to dynamic forces in flight. The shroud ring tail can be used with the same assembly of boom and nozzle as the folding fin tail.

The test results indicate that the shroud ring tail, regardless of the type of nose with which it was tested, showed considerably less drag than the folding fin tail and gave the projectile sufficient static stability to warrant expectation of satisfactory performance in flight.

FIGURE 1. 2.36" ROCKET PROJECTILES AS RECEIVED WITH FIN TAILS FOLDED. UPPER PHOTO SHOWS NOSE NO. 32 (1-13/16" DIA.). LOWER PHOTO SHOWS NOSE NO. 31 (2-1/16" DIA.).

FIGURE 2. PROJECTILE WITH FIN TAIL UNFOLDED. NOSE NO. 31. FIN TAIL NO. 5.

1. SCOPE AND PURPOSE OF TESTS

This report covers water tunnel tests on the M-7, 2.36" diameter rocket with folding fin tails and two hemispherical noses of different diameter. The projectiles were submitted to the laboratory by Capt. E. G. Uhl, Ordnance Department, by letter of March 17, 1943.

The purpose of the tests was to ascertain the hydrodynamic characteristics of the projectile with the two different noses submitted and to compare the results with results obtained by testing these noses in combination with ring tail No. 38 on which previous tests had shown satisfactory performance when combined with a conical pointed nose (Nose No. 8). Sections 6 and 7 at the end of this report describe the test installation, the derivation of the force coefficients and the method of representing the test data.

2. DESCRIPTION OF PROJECTILES TESTED

All tests were made on full scale projectiles. The boom, or motor, and the folding fin tail were tested as received. The nose and afterbody as received were not suitable for mounting in the water tunnel and full scale models of these parts were made to suit the mounting requirements.

Figures 1 and 2 show the projectile as received with the two types of nose and with the fin tail folded and unfolded. Figure 3 shows the larger hemispherical nose with the ring tail and Figures 4 and 5 show close ups of the ring tail. Detail drawings of the various noses, the afterbody, the folding fin tail, and the ring tail are included with this report.

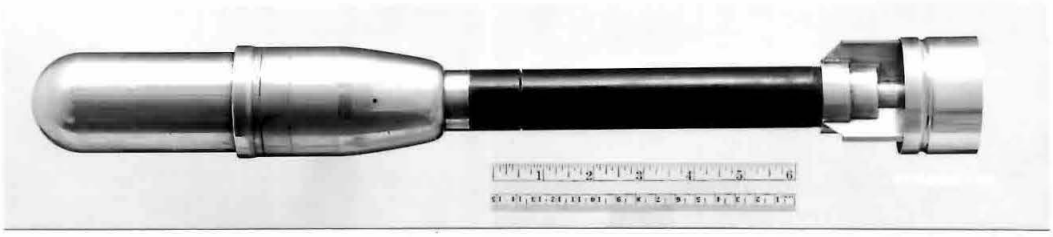

FIGURE 3.
PROJECTILE WITH RING TAIL
NOSE NO. 31. RING TAIL NO. 38

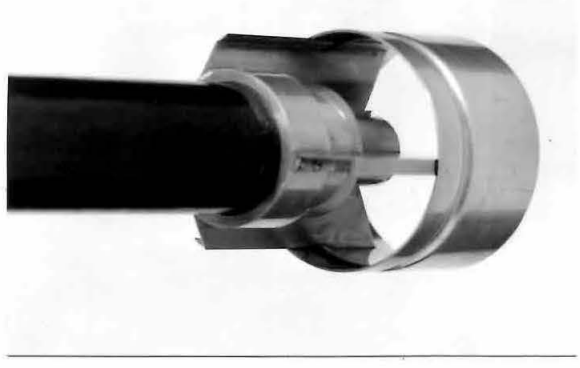

FIGURE 4.
DETAILS OF RING TAIL NO. 38

FIGURE 5.
DETAILS OF RING TAIL NO. 38

3. SUMMARY OF TEST RESULTS

The principal characteristics determined by the tests are summarized in the following tabulation:

Note: All values calculated from the averaged, faired data shown on Figure 15. Length taken as 21.38" for all projectiles tested.

Run No.	Description of Projectile	Drag coefficient at zero yaw C_D	Cross force coefficient at 4 degrees yaw C_C	Moment coefficient at 4 degrees yaw (about center-of-gravity) C_M	Distance from nose to center-of-pressure relative to length, at 4 degrees yaw x'/L	Distance from nose to center-of-gravity relative to length	Distance from C.P. to C.G. relative to length at 4 degrees yaw
22	2-1/16" Hemisph. Nose #31 Folding Fin Tail #5	0.46	0.37	-0.085	0.63	0.42	+0.21
23	1-13/16" Hemisph. Nose #32 Folding Fin Tail #5	0.54	0.37	-0.085	0.64	0.42	+0.22
32	Conical Pointed Nose #8 Folding Fin Tail #5	0.42	0.37	-0.092	0.68	0.44	+0.24
73	2-1/16" Hemisph. Nose #31 Ring Tail #38	0.38	0.20	-0.022	0.50	0.41	+0.09
74	1-13/16" Hemisph. Nose #32 Ring Tail #38	0.44	0.20	-0.022	0.51	0.41	+0.10
75	Conical Pointed Nose #8 Ring Tail #38	0.37	0.20	-0.022	0.53	0.43	+0.10

From the above table the following comparisons are to be noted:

1. The drag with the folding fin tail is greater than with the ring tail.

2. The static stability, i.e., the tendency of the hydrodynamic forces to restore the axis of the yawed projectile to the line of flight, is greater with the folding fin tail than with the ring tail.

3. Of the two hemispherical ogive noses submitted, the larger nose (No. 31) shows the lower drag with whichever tail it was tested. The conical pointed nose (No. 8) shows less drag than either of the other noses.

4. The stability, as indicated by the moment coefficient and the location of the center-of-pressure, is slightly greater for the conical nose than for either of the hemispherical noses in tests with the folding fin tail, but in tests with the ring tail, the stability is not materially affected by the type of nose.

4. STUDIES IN POLARIZED LIGHT FLUME

Figures 6 to 12 inclusive are drawings of flow patterns made from observations of the fluid motion about the projectiles in the polarized light flume. The fluid in the flume has asymmetrical physical and optical properties which permit observation of the flow lines when viewed through polarizing plates. The pictures are for flow velocities below the range of the water tunnel experiments and the patterns can be considered only qualitative.

For the flume observations, the ring tail assembly of nozzle, vanes, and shroud was made of lucite in order to render visible the flow pattern inside the shroud.

Comparison of Figures 6 and 7 indicates the reason why nose No. 31 gives a higher drag coefficient than nose No. 32. The maximum diameter of the projectile head is at the junction of the nose and the afterbody. There is an abrupt change in diameter at that point forming an annular surface perpendicular to the flow. The flow patterns indicate a greater disturbance at this point for nose No. 32 than for nose No. 31. If constructional requirements permit a rounding off of this abrupt shoulder as indicated in the sketch, it is quite apparent that the drag of nose No. 32 could be reduced to compare more

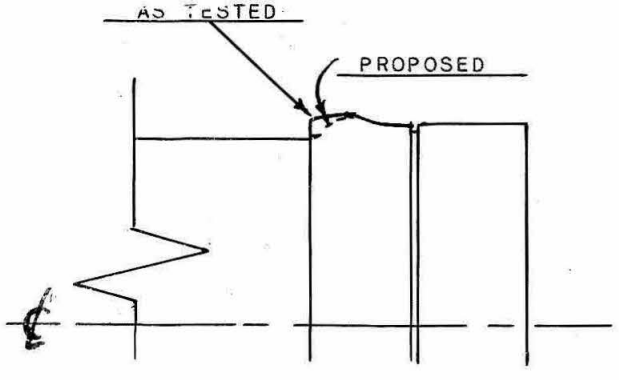

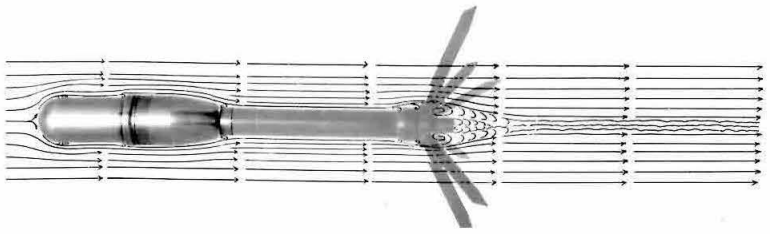

FIGURE 6.
FLOW PATTERN AT ZERO YAW. NOSE NO. 31, TAIL NO. 5. DRAWING BASED ON OBSERVATIONS OF ACTUAL FLOW.

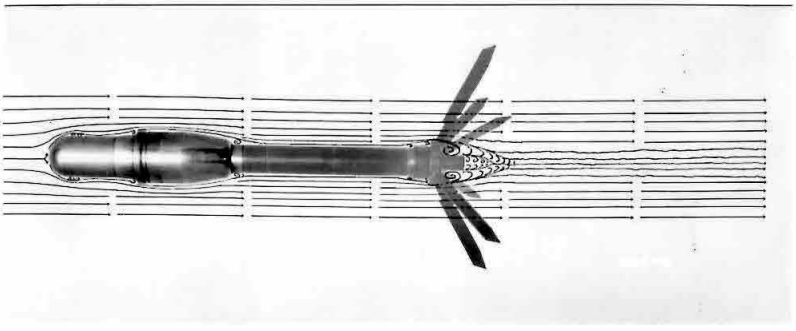

FIGURE 7.
FLOW PATTERN AT ZERO YAW. NOSE NO. 32, TAIL NO. 5. DRAWING BASED ON OBSERVATIONS OF ACTUAL FLOW.

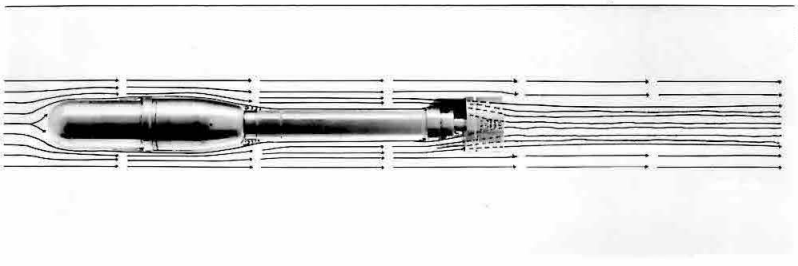

FIGURE 8.
FLOW PATTERN AT ZERO YAW. NOSE NO. 31, RING TAIL NO. 38. DRAWING BASED ON OBSERVATIONS OF ACTUAL FLOW.

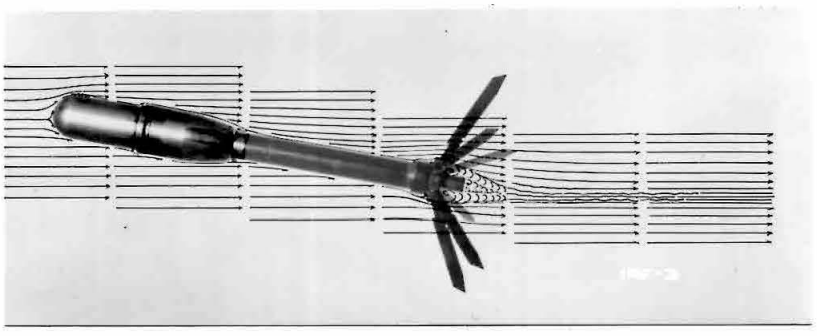

FIGURE 9. FLOW PATTERN AT ABOUT 10 DEGREE YAW. NOSE NO. 31, TAIL NO. 5. DRAWING BASED ON OBSERVATIONS OF ACTUAL FLOW.

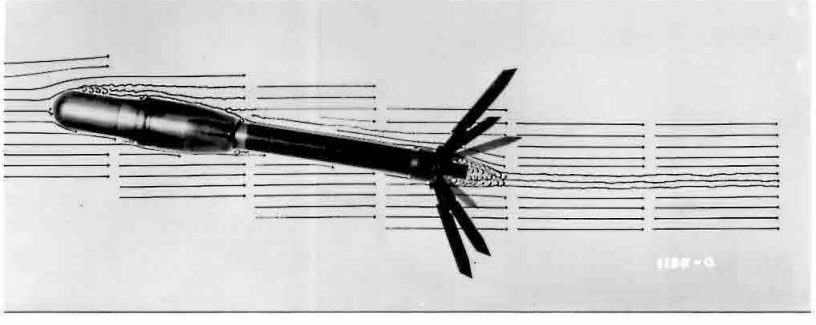

FIGURE 10. FLOW PATTERN AT ABOUT 10 DEGREE YAW. NOSE NO. 32, TAIL NO. 5. DRAWING BASED ON OBSERVATIONS OF ACTUAL FLOW.

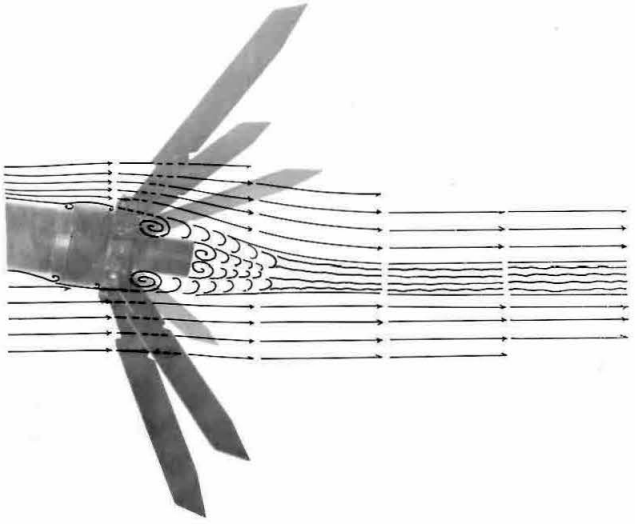

FIGURE 11.
FLOW PATTERN PAST FOLDING FIN TAIL NO. 5 AT ABOUT 10 DEGREES YAW. DRAWING BASED ON OBSERVATIONS OF ACTUAL FLOW.

FIGURE 12.
FLOW PATTERN PAST RING TAIL NO. 38 AT ABOUT 10 DEGREES YAW. DRAWING BASED ON OBSERVATIONS OF ACTUAL FLOW. THE SHROUD OF THE TAIL WAS MADE OF LUCITE SO THAT THE FLOW INSIDE THE TAIL WAS VISIBLE.

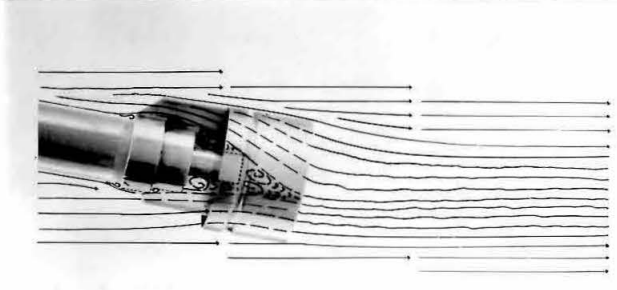

favorably with nose 31, and it is possible that the drag of nose 31 would be slightly reduced.

Figures 9 and 10 show, for about 10 degrees yaw, an even more marked difference in the flow pattern between noses 31 and 32.

Figure 12 shows the wake produced at about 10 degrees yaw through ring tail No. 38. Comparison with Figure 11, which shows the large wake produced by the ring to which the folding fins were attached, serves to explain the large difference in drag between the ring tail and the fin tail. The diameter of the region of disturbed flow or wake is a measure of the amount of drag. The full scale diameter of the disturbed region for the fin tail is about 1-3/4" as against about 5/8" for the ring tail.

5. DISCUSSION OF TEST RESULTS

The values, as calculated from the observed test data, of the drag coefficient, C_D, the cross force coefficient, C_C, the moment coefficient, C_M, and the center-of-pressure location, x/L, plotted against yaw angle, are shown in Figure 13 for test runs Nos. 22 and 73. The curves connecting the C_C and C_M test points do not pass through zero, and the values of x/L and C_D are not the same for corresponding positive and negative yaw angles. This indicates a certain amount of asymmetry in the models. It is seen to be more marked for the folding fin tail than for the ring tail. All of the tests plotted show similar effects of asymmetry. Runs 22 and 73 were selected as illustrative and as showing directly the difference in characteristics between the folding fin tail and the ring tail.

Figures 14 and 15 show a comparison of profiles and force characteristics for all the models covered by this report. The curves of Figure 15 are shown for positive yaw angles only, and were obtained by averaging values for corresponding positive and negative yaw angles and drawing faired curves through the resulting points. (1)

The tests on the folding fin tail models were all made at a velocity in the water tunnel of 20.7 ft/sec. and for the ring tail models at 30.7 ft/sec. It was found that at water velocities higher than about 21 ft/sec., there was considerable fluttering of the fins. At the start of one of the runs one

(1) Figures refer to references listed at end of this report.

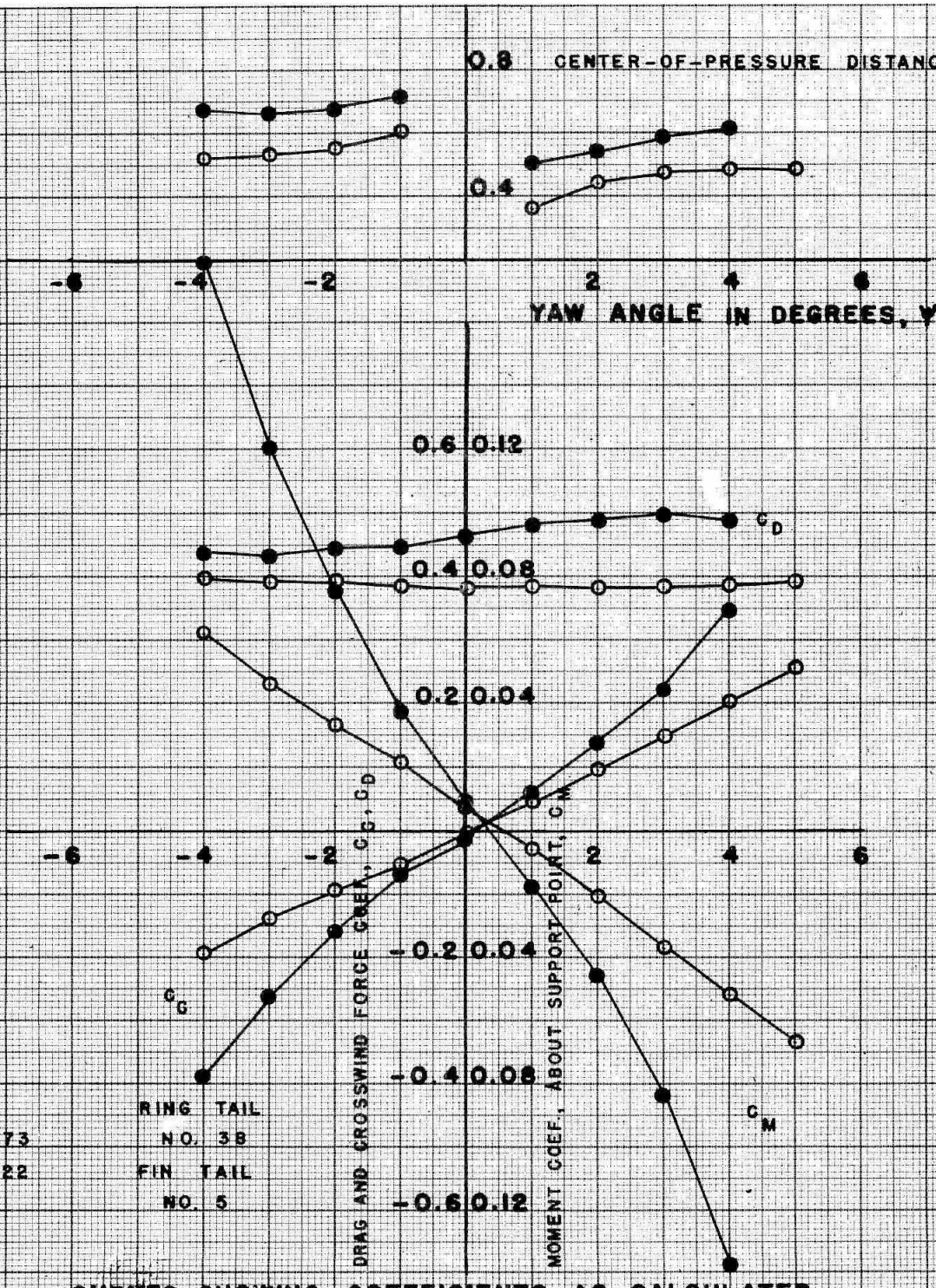

CURVES SHOWING COEFFICIENTS AS CALCULATED DIRECTLY FROM TEST OBSERVATIONS

THE HIGH SPEED WATER TUNNEL
AT THE
CALIFORNIA INSTITUTE OF TECHNOLOGY
SHEET NO. ND11,945 L RUNS 22, 73
PRINT NO. _____ TESTS APRIL - JUNE 1943

FIG. 13

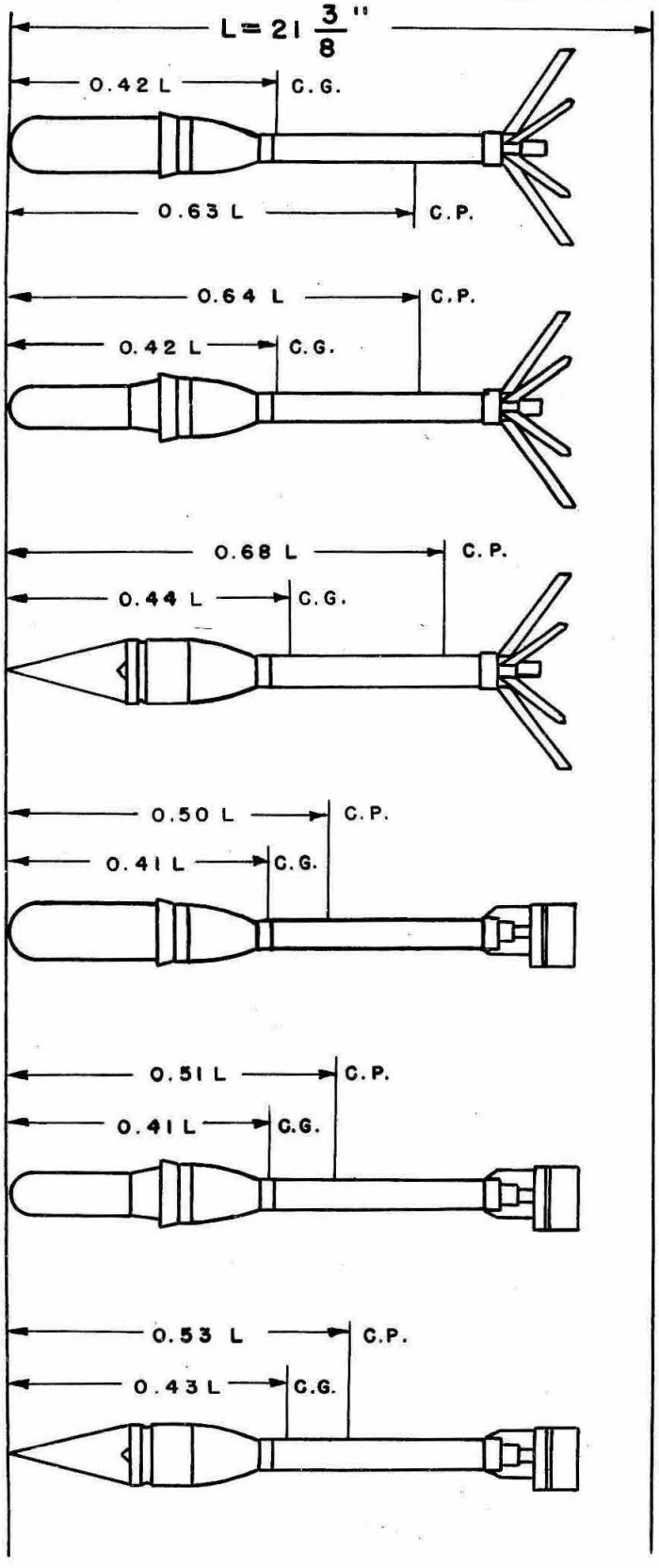

HYDRAULIC MACHINERY LABORATORY CALIFORNIA INSTITUTE OF TECHNOLOGY		
DR	2.36" ROCKET PROJECTILES SHOWING C.G. & C.P. LOCATIONS	SCALE
CH		
AP	DRAWN TO SCALE	ND11-958-L

FIG 14

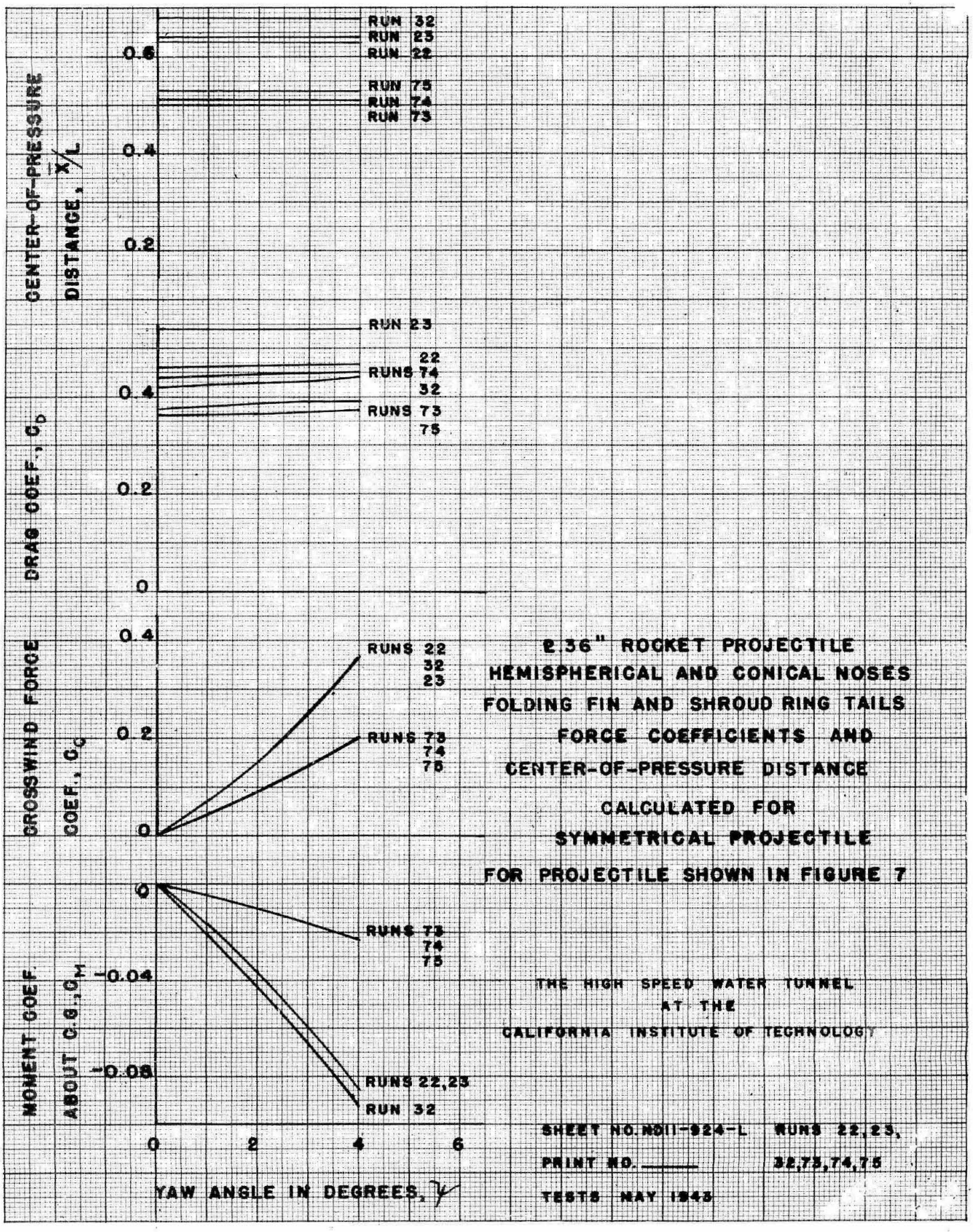
CENTER-OF-PRESSURE DISTANCE, $\bar{X}/L$
RUN 32
RUN 23
RUN 22
RUN 75
RUN 74
RUN 73
0.6
0.4
0.2
0
DRAG COEF., C_D
RUN 23
22
RUNS 74
32
RUNS 73
75
0.4
0.2
0
CROSSWIND FORCE COEF., C_C
RUNS 22
32
23
RUNS 73
74
75
0.4
0.2
0
MOMENT COEF. ABOUT C.G., C_M
0
RUNS 73
74
75
-0.04
-0.08
RUNS 22,23
RUN 32
0
2
4
6
YAW ANGLE IN DEGREES, γ
2.36" ROCKET PROJECTILE
HEMISPHERICAL AND CONICAL NOSES
FOLDING FIN AND SHROUD RING TAILS
FORCE COEFFICIENTS AND
CENTER-OF-PRESSURE DISTANCE
CALCULATED FOR
SYMMETRICAL PROJECTILE
FOR PROJECTILE SHOWN IN FIGURE 7
THE HIGH SPEED WATER TUNNEL
AT THE
CALIFORNIA INSTITUTE OF TECHNOLOGY
SHEET NO. NOII-924-L
PRINT NO. _____
RUNS 22,23,
32,73,74,75
TESTS MAY 1945

FIG. 15

fin was in the folded position and remained folded when the velocity was brought to 20 ft/sec. The velocity was increased momentarily to 30 ft/sec. in order to unfold the fin. However, the fin failed before unfolding, being bent backward about 90 degrees. The corresponding air velocities for equal forces are approximately 600 and 900 ft/sec. This indicates a certain unreliability which is apparent from the rather fragile construction of the fins and their attachment. Fin failure in flight would result in erratic behavior and possible tumbling.

The projectiles were received with the heads weighted to correspond with the weight distribution after the propellant is completely burned. The location of the center-of-gravity was determined by balancing the projectile as received and modified by calculation when the ring tail was substituted for the folding fin tail.

Moving the center-of-gravity forward is a direct means of increasing stability and any possibility of accomplishing this should be carefully considered in the design of the rocket. This is emphasized by the diagrams on Figure 14, particularly for run No. 75, which shows x/L at maximum value but the effect is canceled by the shift of the center-of-gravity.

Tests of other ring tails, not covered in this report, indicate that substantially lower drag coefficients can be obtained, but at some sacrifice in stability. If low drag is of value, further tests are desirable on other types of tails with the objective of devising a tail shape which will give a lower drag together with satisfactory stability.

6. TUNNEL INSTALLATION AND DESCRIPTION OF FORCES MEASURED.

The tests were conducted in the 14" diameter working section of the High Speed Water Tunnel at the California Institute of Technology. (2) Figure 16 shows a projectile installed in the tunnel. In order to reduce the drag tare to a minimum, the rigid supporting spindle is protected from the flow by the streamline shielding shown in the figure. This shielding, which projects to within a few thousandths of an inch of the projectile, is held to a small size in order to reduce interference effects.

The forces exerted by the flow on the model can be resolved, in general, into a drag force parallel to the flow, a cross wind force normal to the flow and a moment or torque acting about the point of support. These are the forces measured during the tests. The moment exists only if the model is not supported at the point of application of the resultant of all the hydrodynamic

(2) **Figures refer to references listed at the end of this report.**

forces. It is clear that the magnitude and sense of the measured moment will change if the point of support is shifted along the body.

The data presented in this report have not been corrected for scale effect, tare, or interference of the model support. However, the results are believed to be close to the correct values. Similar tunnel tests of streamlined projectiles have given data that agree closely with those obtained from full scale field tests. The Water Tunnel test results are applicable in air as well as in water for velocities below that of sound. For air velocities in the neighborhood or above that of sound, the results will not apply.

7. REPRESENTATION OF TEST DATA.

The hydrodynamic characteristics are presented in the form of curves of force coefficients as functions of the angle of yaw. In addition, the distance of the center-of-pressure from the nose of the projectile expressed as a fraction of the length of the projectile is plotted against yaw angle. The center-of-pressure is defined as the point at which the resultant hydrodynamic force vector intersects the axis of symmetry of the model.

The force coefficients, C_D, for drag and, C_C, for cross wind force are expressed as :

$$C_D = \frac{D}{\rho \frac{V^2}{2} A_D}$$

and

$$C_C = \frac{C}{\rho \frac{V^2}{2} A_D}$$

where

D = measured drag force in lbs
C = measured cross wind force in lbs
ρ = density of water in slugs per cu ft
A_D = area in sq ft of a cross section at the cylindrical portion of the projectile taken normal to the geometric axis of the projectile (= 2.98 sq in, i.e. dia = 2.25" for this projectile)

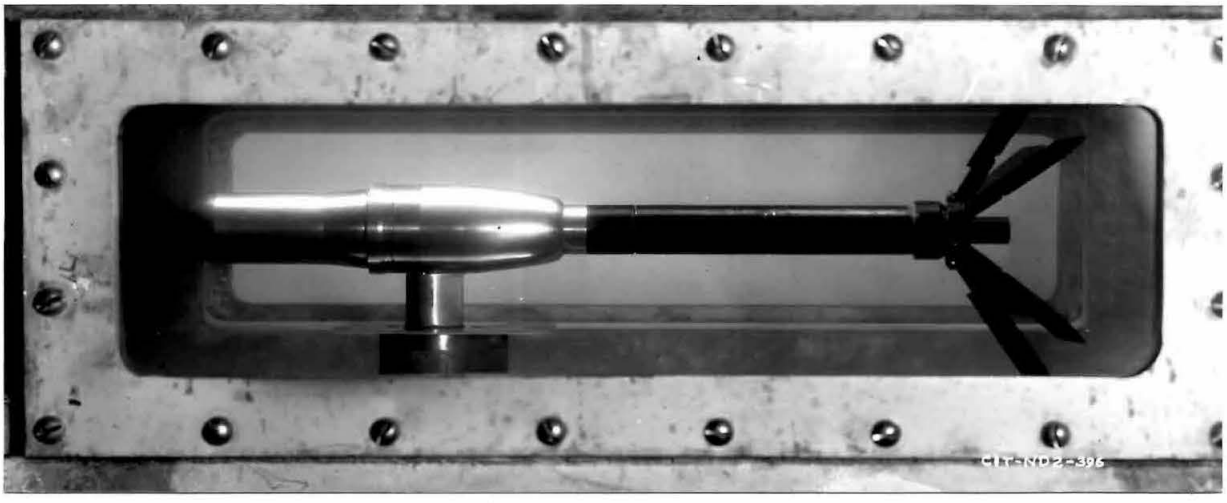

FIGURE 16. 2.36" ROCKET PROJECTILE SHOWN MOUNTED IN THE WATER TUNNEL WORKING SECTION. NOSE NO. 32, FIN TAIL NO. 5.

The moment coefficient is expressed as :

$$C_M = \frac{M}{\rho \frac{V^2}{2} A_D L}$$

where

M = moment in in-lbs measured about any particular point on the geometric axis of the projectile

L = overall length of the projectile in in. (For all combinations of the model projectile discussed in this report L is taken as 21.38")

The distance from the nose of the center-of-pressure (center-of-pressure distance) as a fraction of the overall projectile length is expressed as :

$$\frac{x}{L} = \frac{L' + L''}{L} = \frac{L'}{L} + \frac{M}{L(C \cos \psi + D \sin \psi)}$$

where

L' = distance in in from the projectile nose to the center of moments

L" = distance in in from the center-of-pressure to the center of moments

ψ = yaw angle in degrees

When M is the measured moment the center of moments is at the support point of the model and L" then is the distance from the support point to the center-of-pressure. The signs of the moment, M, the cross wind force, C, and the yaw angle, ψ, are such that a positive or clockwise moment will tend to increase a positive or clockwise yaw angle, while the corresponding positive cross wind force will act in the same direction as the displacement of the projectile nose for a positive yaw.

The curves of force and moment coefficients and of center-of-pressure distance plotted as functions of the yaw angle are useful for a discussion of the stability of projectiles. Since these tunnel tests are made under steady flow conditions, the results will only indicate the tendency of the projectile to return to or move away from the equilibrium position after a disturbance. Adopting aerodynamic usage a projectile is said to be "statically" stable if it tends to return to equilibrium

when disturbed. In the discussion of static stability, the actual motion following the perturbation is not considered at all. In fact, a projectile may oscillate about the equilibrium position without ever remaining in it. In this case the projectile would be statically stable even though "dynamically" unstable. For a complete discussion of the mode of motion to be expected following a perturbation, i.e., the "dynamic" stability, additional information is necessary.

The condition for equilibrium is satisfied if C_M calculated about the C.G. is equal to zero. In general, for projectiles with axial symmetry the moment is zero at $\psi = 0^o$ so that for equilibrium the projectile is oriented with its axis parallel to the direction of motion. If the projectile is rotated from the equilibrium position so as to give it a positive yaw angle, it is necessary that it have a negative moment coefficient, according to the sign convention adopted, in order that it be statically stable. Thus a negative slope of the curve C_M vs. ψ corresponds to static stability, and a positive slope corresponds to instability. The degree of stability or instability is measured by the magnitude of the slope. The same conclusions are obtained by interpreting the center-of-pressure curves. For symmetrical projectiles, if the center-of-pressure falls behind the center-of-gravity, a negative or restoring moment exists and the projectile is statically stable. If the C.P. lies ahead of the C.G., the moment is non-restoring and the projectile is statically unstable. The degree of stability or instability is measured by the distance between the center-of-gravity and center-of-pressure.

REFERENCES:

(1) For a discussion of the effects of asymmetry, see "Memorandum of Water Tunnel Tests of a 21-3/8" Rocket Projectile" by R. T. Knapp, Report No. ND-11, Nov. 19, 1942.

(2) For complete description see the following report on file in the office of Section 6.1, NDRC, "The High Speed Water Tunnel at the California Institute of Technology", by R. T. Knapp, V. A. Vanoni, and J. W. Daily, June 29, 1942.

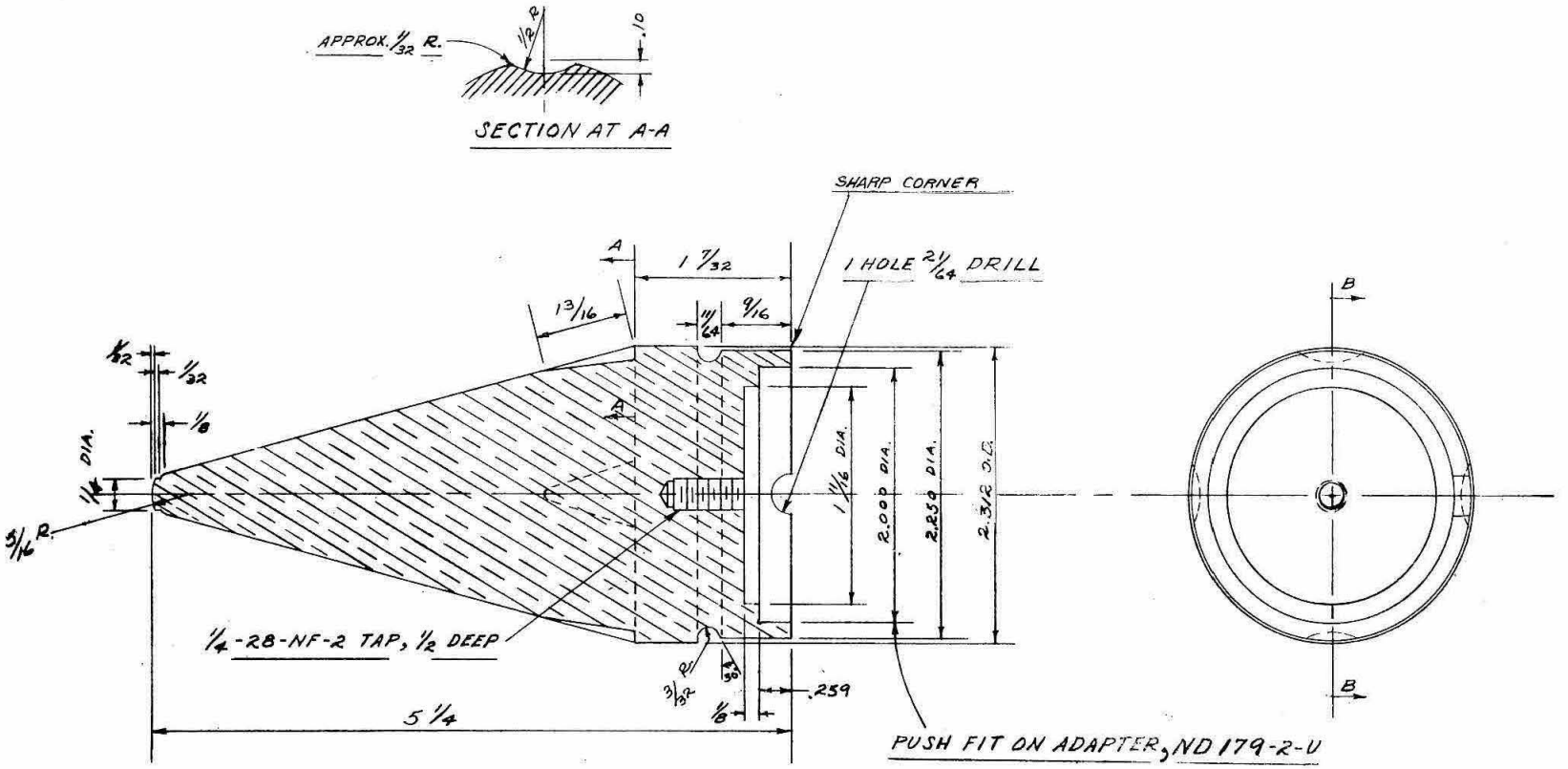

MAT'L ~ BRASS

HYDRAULIC MACHINERY LABORATORY C.I.T. PASADENA	
MODEL NOSE #8 ~~EOR~~ 2.36 DIA ROCKET PROJECTILE	
DR. C.R.A. 11-16-42	SCALE ~ FULL
CK HB	ND-181-8-U
AP	
PRINT NO.	ISSUED TO

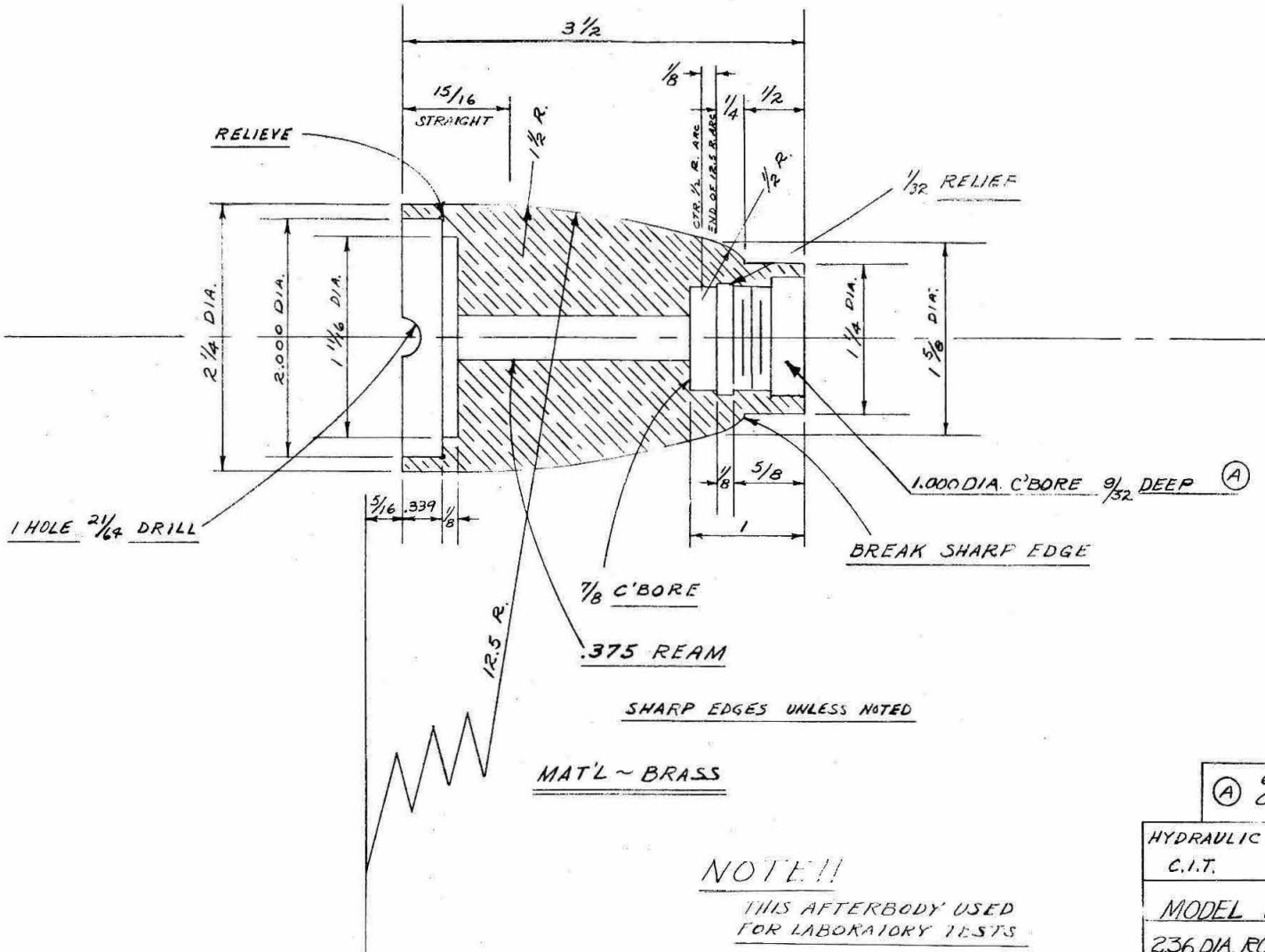

NOTE!!

THIS AFTERBODY USED FOR LABORATORY TESTS

SEE ALSO ND-183-18-U

A 6/26/43 CRA C'BORE ADDED	
HYDRAULIC MACHINERY LAB. C.I.T. PASADENA	
MODEL AFTERBODY #8 FOR 2.36 DIA. ROCKET PROJECTILE	
DR. CRA 11-17-42	SCALE ~ FULL
CK HB	ND-183-9-U
AP 4/8	

PRINT NO. ISSUED TO

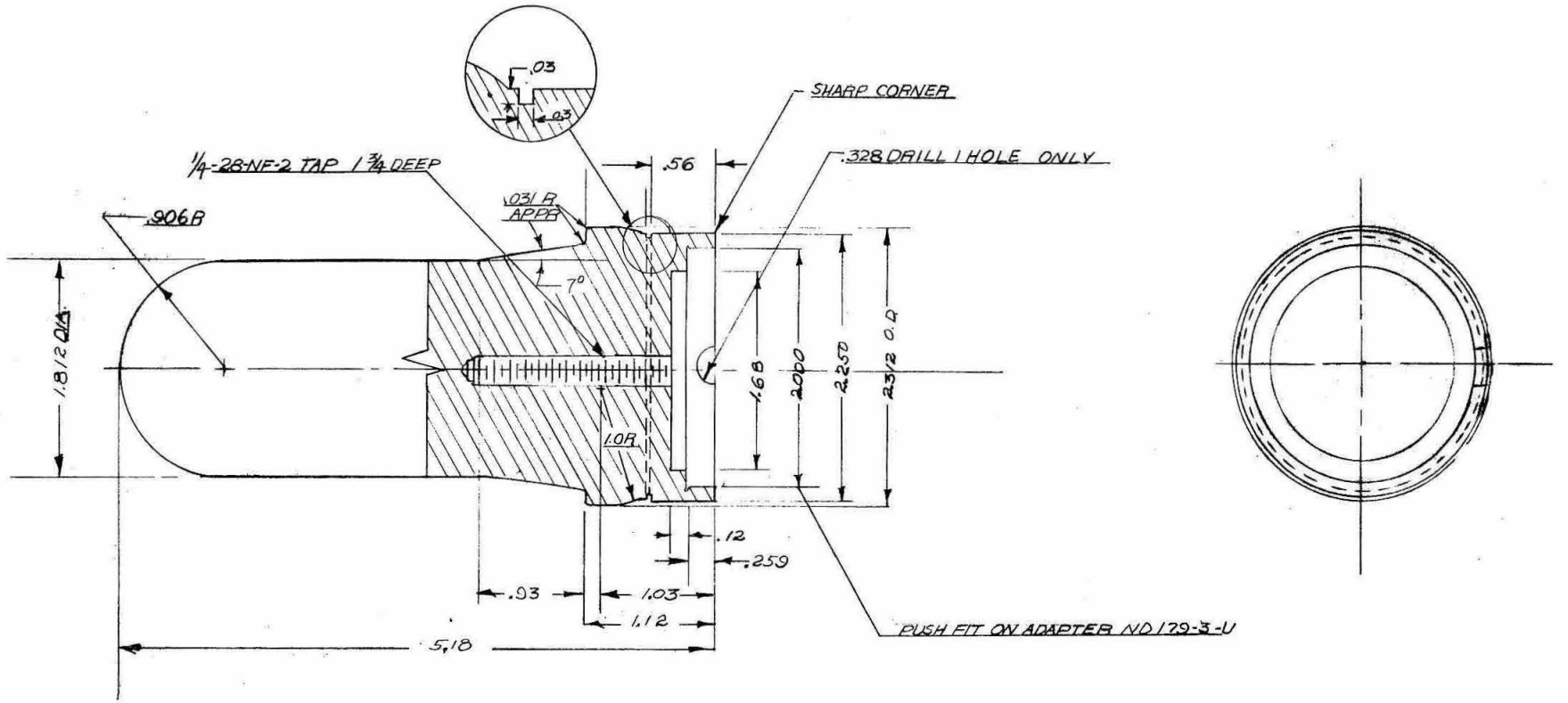

MATERIAL ~ BRASS

HYDRAULIC MACHINERY LABORATORY CALIFORNIA INSTITUTE OF TECHNOLOGY PASADENA, CALIFORNIA	
MODEL NOSE #32 FOR .236 DIA ROCKET PROJECTILE	
DR H.C.Y 4-14-53	SCALE FULL
CH HB	ND 101-32-U
AP [illegible]	
PRINT NO.	ISSUED TO

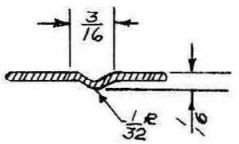

GROOVE DTL.
DOUBLE SIZE

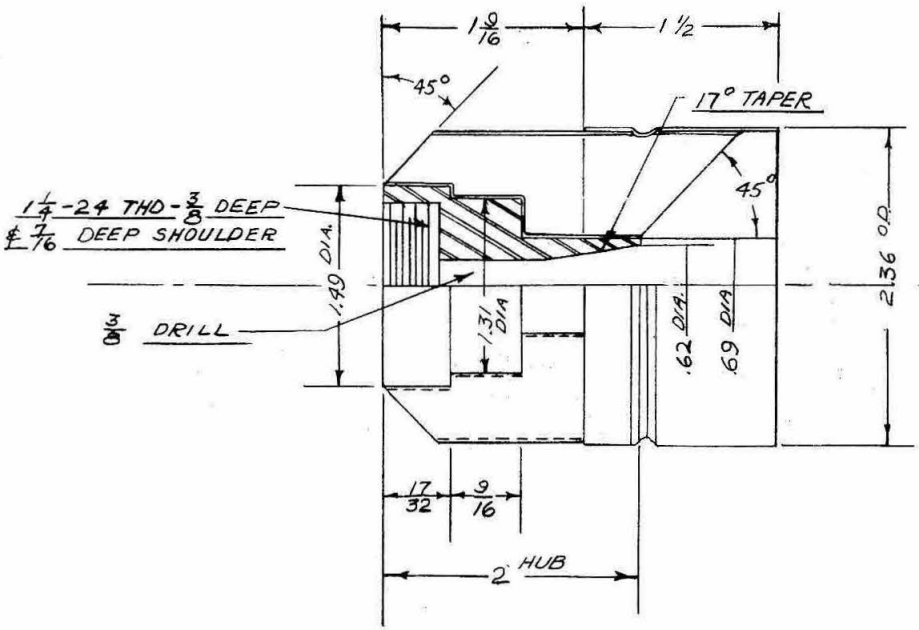

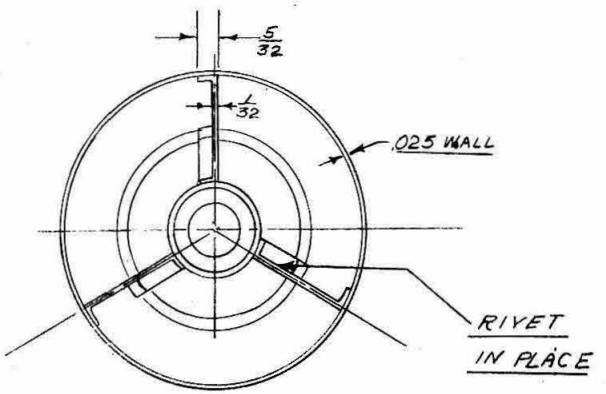

LEAVE SQUARE EDGES
FILLETS TO HAVE .03 R

MAT'L ~ BRASS

NOTE ~ SEE ALSO DRAWING NO. ND-417-421-U FOR GROUP DRAWING OF TAILS 36 THRU 40

HYDRAULIC MACHINERY LABORATORY
CALIFORNIA INSTITUTE OF TECHNOLOGY
PASADENA, CALIFORNIA

MODEL TAIL #38 FOR 2.36 DIA. ROCKET PROJECTILE

DR H.C.Y. 6-23-43	SCALE FULL & NOTED
CH HB	ND-419-U
AP JWA	

PRINT NO. ISSUED TO

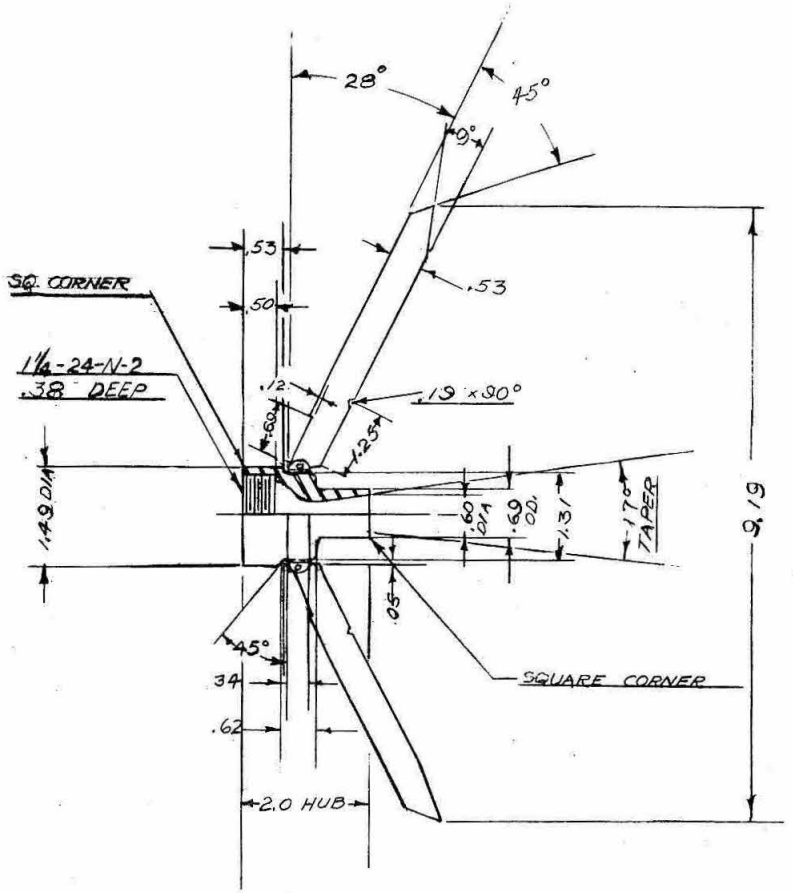

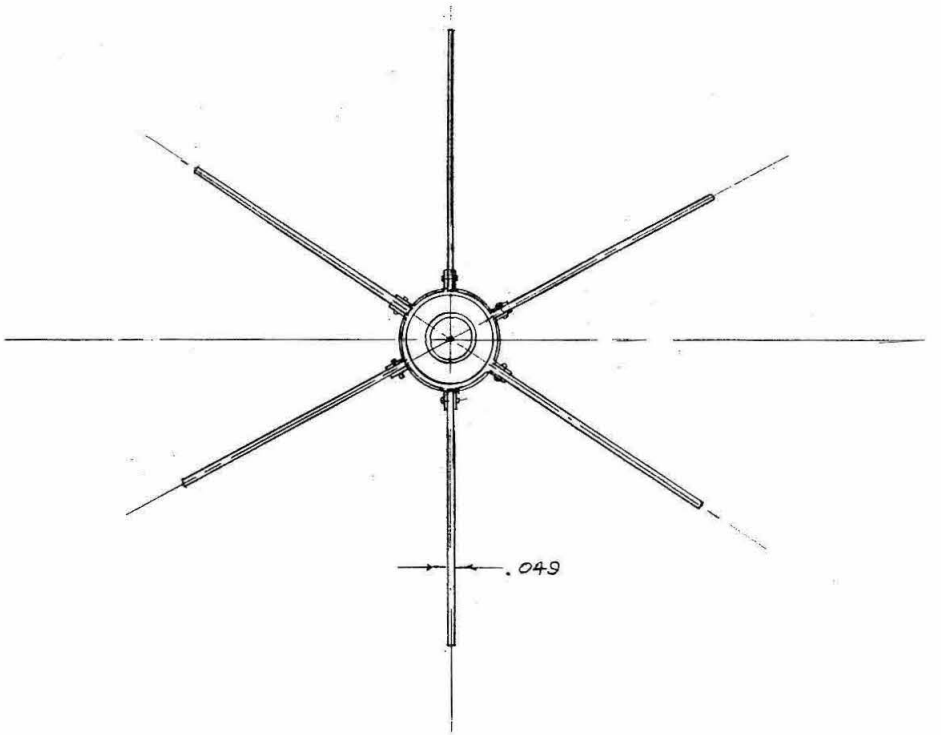

NOTE~ ALL RADII .03 UNLESS NOTED

1/16 FIN RIVETS

FIN ATTACHING RING SPOT WELDED 12 PLACES

HYDRAULIC MACHINERY LABORATORY
CALIFORNIA INSTITUTE OF TECHNOLOGY
PASADENA, CALIFORNIA

FOLDING FIN TAIL #5 FOR 2.36 DIA. ROCKET PROJECTILE

DR H.C.Y. 6/24/43	SCALE HALF
CH HB	NO-427 -U
AP	

PRINT NO. ISSUED TO